Int. Agrophysics, 2008, 22, 5-15

INTERNATIONAL
Agrophysics
www.international-agrophysics.org

Finite element aided brittle fracture force estimation during two-dimensional soil cutting

O.B. Aluko

Department of Agricultural Engineering, Obafemi Awolowo University, Ile-Ife, Nigeria

Received August 6, 2007; accepted December 19, 2007

A b s t r a c t. Short crack behaviour during the two-dimensional cutting of brittle agricultural soils is a non-symmetrical mixed mode crack loading problem. The inability to resolve this problem limited the brittle fracture soil cutting theory developed earlier by Aluko and Chandler (2004). In this paper, finite element modelling was used to simulate the loading of a brittle soil, in which a horizontally propagating crack had been initiated, by a two-dimensional plane cutting blade. Using a finite element subroutine, solutions were obtained for the separate values of the modulus ($\overline{K}$), mode I (K_I) and mode II (K_{II}) stress intensity factors for both short and long crack regimes.

Further analysis of the stress intensity factor curves led to two possible interpretations for estimating peak soil cutting forces: the *energy* criterion and the *direct mode I* criterion. Using both criteria, brittle fracture force predictions were carried out for polished plane cutting blades in a sandy loam and a clay loam soil. The *energy* criterion was found to under-predict soil cutting forces when compared with published experimentally measured forces on these soils. However, the direct *mode I* criterion gave reasonable force estimates compared to measured values over a limited range of low rake angles. In conjunction with the passive pressure theory, the brittle fracture model can be used to predict the expected soil failure mechanism in a given situation by applying the minimal energy criterion in the comparison of forces predicted by both theories.

K e y w o r d s: soil fracture, crack growth, finite element method, blade configuration, soil cutting forces

INTRODUCTION

The mechanism of brittle fracture, which sometimes occurs during soil cutting and tillage operations, is not yet fully understood. Previous work by Aluko and Seig (2000) showed that the fracture of brittle agricultural soils during two-dimensional cutting operations is principally an elastic problem. Aluko and Chandler (2004) subsequently developed a model for brittle fracture during two-dimensional soil cutting, using methods of fracture mechanics for elasticbrittle materials. The estimation of maximum cutting forces with the use of the model was, however, limited because of inability to deduce short crack behaviour under mixed mode loading.

The finite element method (FEM) has been used as an approximate numerical solution procedure for solving many kinds of linear and non-linear continuum mechanics problems. In particular, in soil mechanics research work, it has been pointed out (Coleman and Perumpral, 1974) that the method is capable of providing information which is difficult or sometimes impossible to obtain experimentally; and in the present work, by the previous theoretical approach (Aluko and Chandler, 2004; Coleman and Perumpral, 1974; Perumpral *et al*., 1971; Raper and Erbach, 1990, and Yong and Fattah, 1976) have applied the FEM to the study of soil compaction and the associated deformation and stress distribution patterns within a soil under the influence of a tractor wheel or other compaction device. Yong and Hanna (1977) modelled soil cutting by simple plane (two-dimensional) blades using the FEM. Liu Yan and Hou Zhi-Min (1985) and Chi and Kushwaha (1987, 1989) applied the FEM to the study of three-dimensional soil cutting with narrow blades. Using finite element modelling, Fielke (1999) studied the effect of different tillage tool cutting edge geometries on the deformation, forces and soil movement around the cutting edge.

In the foregoing applications of the FEM, soil mechanical behaviour was modelled based on the classical Mohr-Coulomb theory of shear failure. In general, this approach is appropriate for processes where deformation (or plasticity effects) is significant. Examples of such processes include wheel-soil interaction, triaxial testing and mole ploughing.

Corresponding author's e-mail: elbeeluxe@yahoo.com

It is also appropriate in the analysis of soil cutting problems where shear failure with significant plastic deformation occurs. However, it has been shown (Aluko and Seig, 2000; Aluko and Chandler, 2004) that when brittle fracture occurs in soil cutting, soil mechanical behaviour can be macroscopically considered to be elastic-brittle.

To resolve the limitation (pointed out above) of the brittle fracture soil cutting model developed by Aluko and Chandler (2004), this study was carried out to deduce short crack behaviour under mixed mode loading using the FEM and to predict brittle fracture forces during two-dimensional soil cutting.

BRITTLE FRACTURE SOIL CUTTING THEORY

For an ideally horizontally propagating crack in a brittle agricultural soil (Fig. 1), Aluko and Chandler (2004) showed that the fracture process leading to clod formation comprises two regimes of crack growth/development, termed the *short* and *long* crack regimes. During the initial stages of crack growth in the short crack regime, the relationship between the developing crack and the applied cutting force is given by (Aluko and Chandler, 2004):

$$\frac{K_I}{H}\left[\frac{a(\pi^2-4)}{4\pi}\right]^{1/2}=\frac{V}{H}-\frac{2}{\pi}, \qquad (1)$$

where: K_I is the applied stress intensity factor (N m$^{-3/2}$), V and H are the vertical and horizontal components, respectively, of the cutting force P in N exerted on the soil by the blade (Fig. 1), and a is the crack length (m). With further development, crack behaviour changes from short to long. The model for long crack behaviour (Aluko and Chandler, 2004) is:

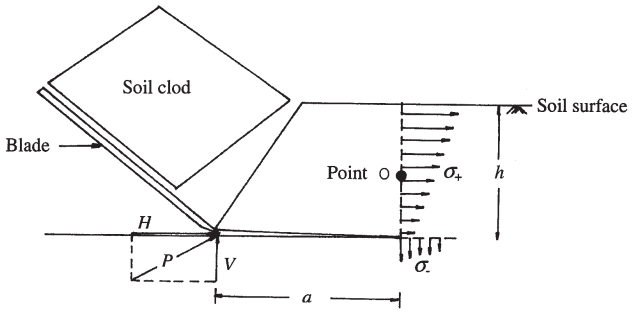

Fig. 1. Schematic illustration of the brittle fracture model for two-dimensional soil cutting: P – cutting force exerted by the blade, H — horizontal component of force P, V – vertical component of force P, a – crack length, h – height of encastré soil beam above developing crack; σ_+ – compressive stress, σ_- – tensile stress.

$$\frac{K_I h^{1/2}}{H}=-0.541+1.68\left(\frac{V}{H}\right)+1.92\left(\frac{V}{H}\right)\left(\frac{a}{h}\right), \qquad (2)$$

where h is the height (m) of the encastré soil beam above the developing crack.

The pattern of applied stress intensity factors for both short and long crack models is illustrated in Fig. 2 for different values of V/H between 1 and $2/\pi$. Aluko and Chandler (2004) attributed the apparent incompatibility between the two models (Fig. 2) to the difference in their modes of crack loading. Whereas the derivation of the short crack model was based on conditions of symmetrical single mode crack loading, that of the long crack model was based on non-symmetrical mixed mode crack loading. As pointed out earlier, this paper reports the use of the finite element method to deduce short crack behaviour during the two-dimensional cutting of brittle agricultural soils, which constitutes a non-symmetrical mixed mode crack loading problem.

FINITE ELEMENT MODELLING

To deduce short crack behaviour during two-dimensional soil cutting, finite element modelling was used to simulate the loading of a brittle soil, in which a horizontally propagating crack had been initiated, by a two-dimensional plane cutting blade. The study was carried out using subroutines from a finite element modelling software (Henshell, 1984). As pointed out by Fielke (1999), in the application of finite element modelling it is assumed that the material, in this case soil, consists of discrete connected elements with assigned material properties on which displacement and force constraints are applied.

Geometric boundary conditions

In the present application of the finite element method, the geometrical configuration and boundary conditions were chosen to simulate the actual experimental soil and blade conditions previously reported by Aluko and Seig (2000). Figure 3 shows the finite element idealization of the blade-soil system. The system consisted of an inclined plane (two-dimensional) blade cutting through a soil continuum having a height of 163 mm and a width of 700 mm. Blade working depth h was kept constant at 70 mm below the soil surface while different blade rake angles within the range 25-90° were investigated. The soil surface was assumed to be horizontal and stress free, and blade motion was assumed to be horizontal. At a sufficiently large horizontal distance from the blade tip ($x = 10h$), the front side boundary was chosen so that there was no displacement of soil elements in the x-direction. The same obtained for the rear side boundary below the developing crack. It was also assumed that at a reasonable depth below the crack line ($y = 1.3h$), vertical movements of soil elements were vanishingly small at the bottom boundary of the soil continuum.

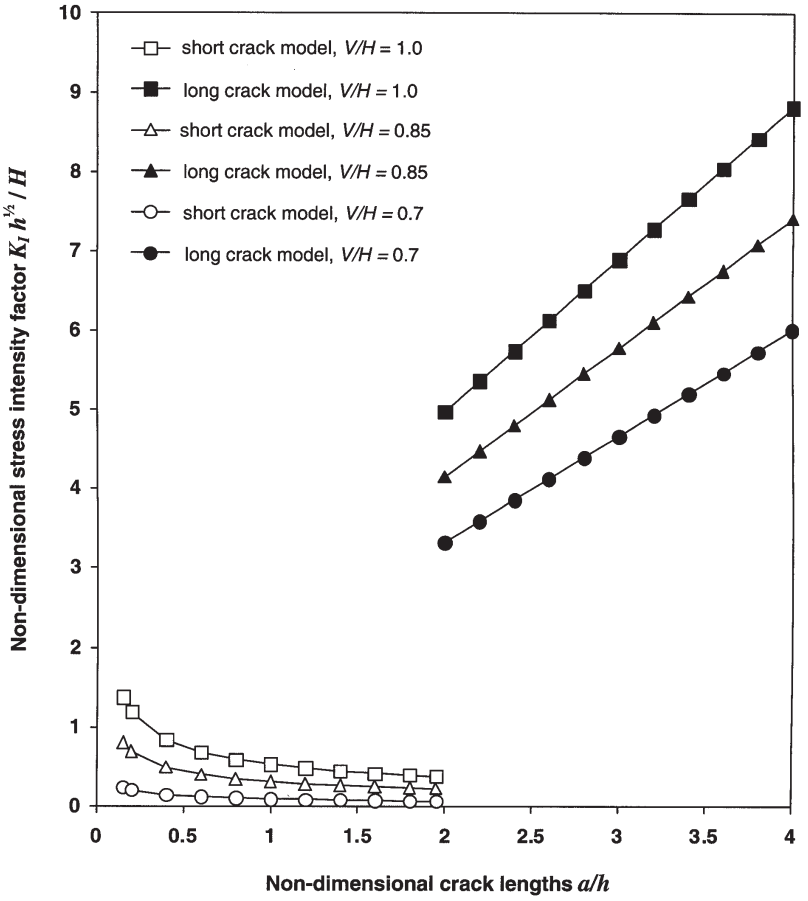

Fig. 2. Typical stress intensity factor curves for short and long crack models: K_I – applied stress intensity factor, h – height of encastré soil beam above crack tip, a – crack length, H – horizontal component of cutting force P exerted by the blade, V – vertical component of cutting force P exerted by the blade (Aluko and Chandler, 2004).

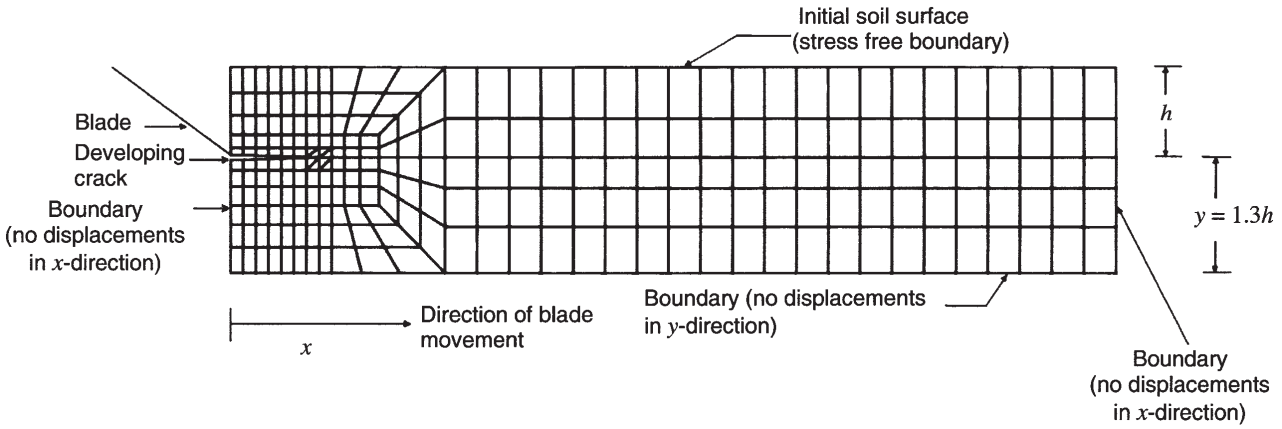

Fig. 3. Finite element idealization of the blade-soil system and developing crack.

Discretization and element specification

The overall discretization of the soil continuum is shown in Fig. 3. Deformations and strains were accounted for by the use of isoparametric elements in preference to linear constant strain triangular elements. The latter have often been used in previous applications for the finite element meshes except at points of slip and failure. Figures 4a and 4b show a typical linear constant strain triangular element and isoparametric elements, respectively. The advantages of the isoparametric element over the linear constant strain triangular element are two-fold:

1. The element uses a polynomial interpolation for the displacements over the element whereas a linear interpolation is carried out for the linear constant strain triangular element. Whilst the element sides in the latter always remain straight, the former accommodates reasonable distortions from the straight-sided configuration and element sides can be curved. This makes the isoparametric element concept very powerful. In the analysis of a body with curved boundaries or where geometric non-linearity may occur due to deformation, the use of a large number of straight-sided constant strain triangular elements can be avoided by using isoparametric elements. Better accuracy of results is also generally obtained.

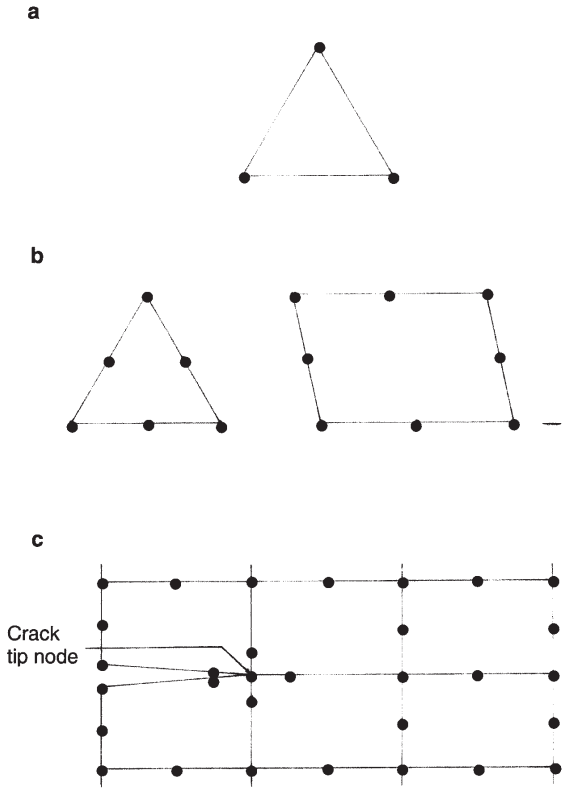

Fig. 4. Element types and crack tip modelling: a – three-noded linear constant strain triangular element, b – six and eight-noded isoparametric elements, and c – isoparametric distortion for crack tip singularity.

2. Isoparametric distortion makes this element very suitable for the modelling of singularities in the region of a crack tip. This is achieved by moving the mid-side nodes of element sides adjacent to the crack tip, from their usual position at the centre of each side to $\frac{1}{4}$ the element side from the crack tip node. The procedure is illustrated in Fig. 4c. Crack tip stress intensity factors can be accurately determined using this procedure. The mathematical justification for this procedure can be found in Zienkewicz (1971) and Henshell (1984).

Figure 5 depicts the crack tip region of Fig. 3 enlarged. Although the nodes are not shown, the triangular elements that were used to model soil in the immediate vicinity of the crack tip in Fig. 5 were six-noded isoparametric elements of the type shown in Fig. 4b. This was in accordance with the requirements for crack tip modelling of the finite element software used. Eight-noded quadrilateral isoparametric elements were used elsewhere within the finite element mesh.

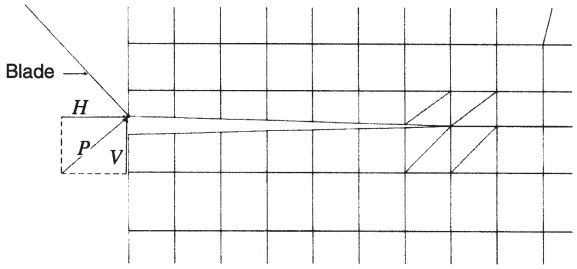

Fig. 5. Element specification, modelling and loading of the crack tip region of Fig. 3 (enlarged).

Soil properties

The input soil properties for the present analysis are the Young's modulus, E, the Poisson's ratio, ν, and the density of the soil. These properties are summarised in Table 1 and were considered to be constant. The Young's modulus was determined from stress-strain curves obtained from triaxial test data on soil samples tested at zero confining pressure or uniaxial compression ($\sigma_2 = \sigma_3 = 0$). The secant modulus at $\frac{1}{3}$ peak stress was taken as the value of Young's modulus, E (Bofinger, 1970). A typical illustration of the secant modulus is shown in Fig. 6. The values of soil dry density used in the present analysis corresponded with those of the experimental soils previously reported by Aluko and Seig (2000).

T a b l e 1. Soil properties used in finite element modelling

Soil property	Sandy loam	Clay loam
Density (Mg m^{-3})	1.33	1.40
Young's modulus (MN m^{-2})	5.521	5.797
Poisson's ratio	0.3	0.3

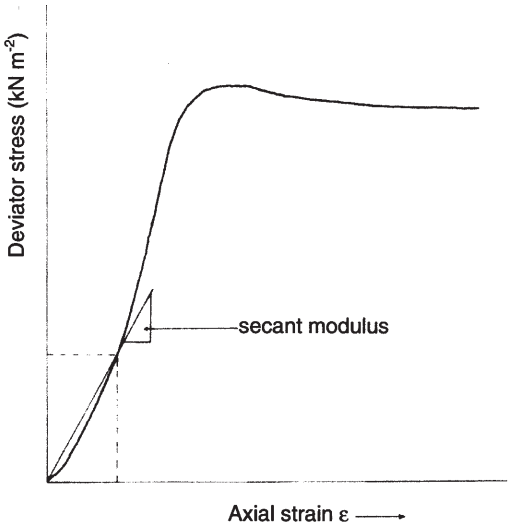

Fig. 6. Schematic illustration of the secant modulus *E*.

Values of Poisson's ratio within the range of 0.25-0.49 have been used by research workers in soil and rock mechanics studies, the lower part of the range being used for more brittle samples whilst the upper part is used for more ductile samples where significant deformations occur. Young's and Hanna (1977) used a value of 0.49, Coleman and Perumpral (1974) used a value of 0.4, and Seig (1985) used a value of 0.25. It has been posited that a Poisson's ratio value of 0.3 is typical for dense top soils (Anonymous, 1990; Fielke, 1999). However, preliminary investigations by Aluko (1988), using different values of Poisson's ratio within the range 0.25-0.49, showed that within this range no significant effect was observed on the values of the applied stress intensity factors obtained. The Poisson's ratio used in the present analysis was therefore kept constant at a value of 0.3.

Load boundary conditions and analytic procedure

Although the cutting force in shear failure results from the continuous development of passive pressures on the surface of the cutting blade, it has been shown (Aluko and Chandler, 2004; Aluko and Seig, 2000) that in brittle fracture the cutting force is cyclic in nature and is essentially concentrated in the region of the blade tip. The brittle fracture cutting force can be resolved into its horizontal and vertical components. In the present finite element analysis, the applied load at the tip of the cutting blade is simulated by specifying constant horizontal and vertical loads on the corner node of the developing crack as shown in Fig. 5. This provides the load boundary conditions. For a particular blade configuration *ie* a constant load ratio *V*/*H*) the analysis proceeds by allowing the crack length to increase by specified constant small increments for each subsequent finite element run. The analytical procedure is illustrated schematically in Fig. 7.

Preliminary analysis and validation of the procedure

Consider Fig. 5. Following the analytical procedure described above and illustrated in Fig. 7, for each crack length the displacements *dx* and *dy* in the horizontal and vertical directions, respectively, of the edge node were obtained from the output results of each finite element run. The strain energy *S* was then determined from the relationship:

$$S = \frac{1}{2}(Hdx) + \frac{1}{2}(Vdy), \tag{3}$$

The energy release rate G could then be determined from:

$$G = dS / da, \tag{4}$$

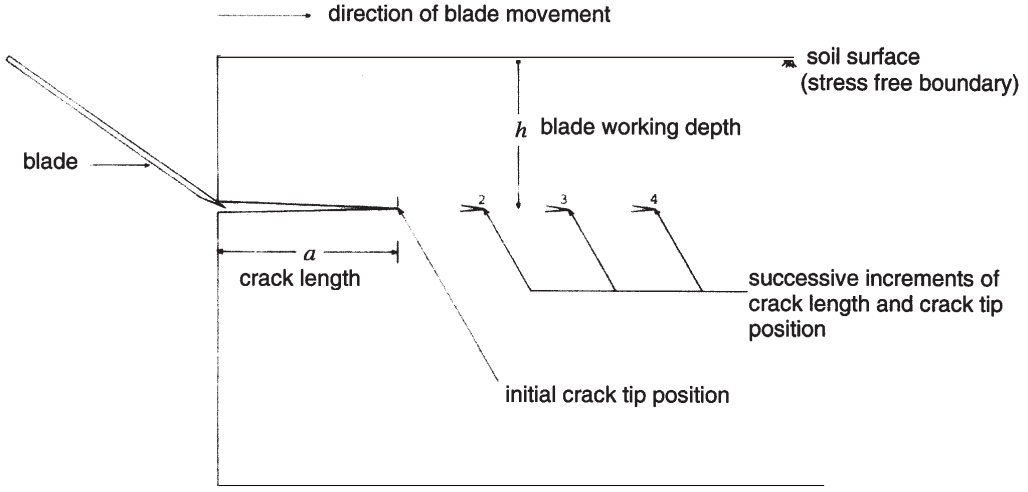

Fig. 7. Schematic illustration of incremental crack length procedure.

where: a is the crack length and dS is the infinitesimal change in strain energy corresponding to an infinitesimal change da in crack length. An interpolation was thus performed for each value of G using the values of S for consecutive runs at different crack lengths, a. Finally, the modulus ($\overline{K}$) of the stress intensity factor was determined from:

$$\overline{K} = \sigma\sqrt{\pi a} = \sqrt{GE}. \quad (5)$$

As pointed out by Aluko and Chandler (2004), for mixed mode problems the relationship between $\overline{K}$, K_I and K_{II} is given by:

$$\overline{K} = \left(K_I^2 + K_{II}^2\right)^{1/2}, \quad (6)$$

where: K_I and K_{II} are the mode I (opening mode) and mode II (sliding mode) stress intensity factors, respectively.

To check the validity of the finite element (interpolation) procedure used, a simple analysis was carried out for a long crack ($a/h > 2$) propagating under the influence of a constant vertical load V applied at the blade tip (Fig. 8).

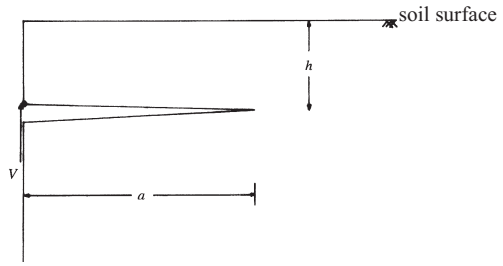

Fig. 8. Long crack (a/h > 2) propagation under a constant vertical load V.

Stress intensity factor ($\overline{K}$) values were determined using Eqs (3), (4) and (5). Since $H = 0$, the term Hdx on the right hand side of Eq. (3) vanishes. The stress intensity factors thus determined were compared with the analytical solutions (predicted values) obtained from the relationships proposed by Cotterell *et al*. (1985). For the case considered, the modulus $\overline{K}$ of the applied stress intensity factor is given by (Cotterell *et al*., 1985):

$$\frac{\overline{K}h^{1/2}}{V} = 1.50 + 2.44\,(a/h), \quad (7)$$

and the mode I stress intensity factor K_I is given by:

$$\frac{K_I h^{1/2}}{V} = 1.68 + 1.92\,(a/h). \quad (8)$$

The predicted values and the finite element values of $\overline{K}$ are presented on a non-dimensional plot as a function of the crack length a in Fig. 9. The predicted values of K_I are also shown. The figure shows very good agreement between the finite element values and the predicted values. This indicates the validity of the finite element (interpolation) procedure used. Using the interpolation procedure, a preliminary analysis of the brittle fracture soil cutting problem (Figs 5 and 7) was carried out to examine the pattern of $\overline{K}$ for load ratios V/H of 0.5, 0.2 and 0.05.

Complete stress intensity factor solutions

It has been pointed out that the soil cutting loads are of mixed mode and Aluko and Chandler (2004, 2006) have shown that the material property that governs brittle fracture by crack opening and propagation is the mode I stress intensity factor K_{Ics} of the soil. Knowledge of the pattern of the mode I applied stress intensity factor K_I in soil cutting is thus required as this will enhance the estimation of soil forces when used in conjunction with experimentally determined values of K_{Ics}. In order to obtain the stress intensity factors for mode I and mode II separately a PAFEC subroutine, the *CRACK.TIP* module, was used. This computes the separate values of K_I and K_{II} from the displacements obtained in the finite element analysis (Henshell, 1984). Using the *CRACK.TIP* module procedure, load ratios (V/H) within the range 0.1-0.8, which represent different blade configurations, were analysed. For each load ratio, several finite element runs were carried out using the incremental crack length method described earlier and stress intensity factor solutions were obtained for K_I, K_{II} and $\overline{K}$.

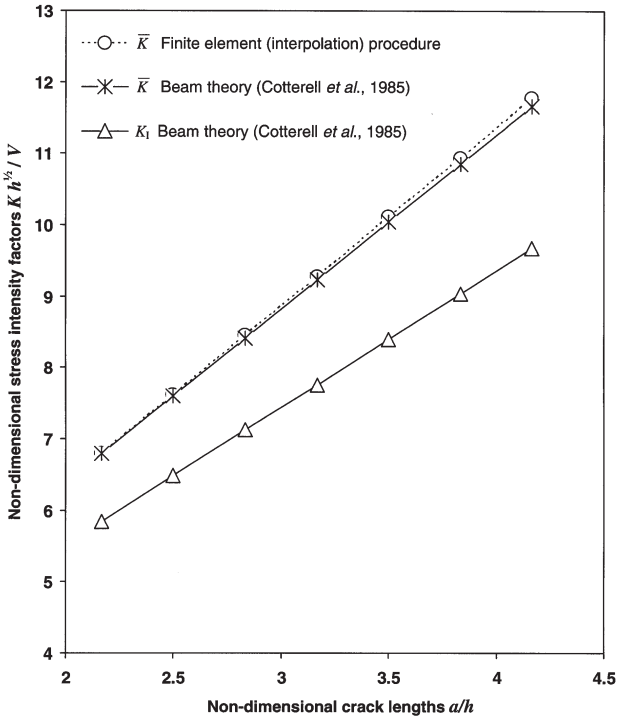

Fig. 9. Comparison of stress intensity factors for long cracks ($a/h > 2$).

RESULTS AND DISCUSSION

Stress intensity factor solutions

The results of the preliminary analysis carried out using the interpolation procedure are shown in Fig. 10. For the practical range of crack lengths considered, $\overline{K}$ initially decreases as the crack grows for V/H ratios of 0.5 and 0.2. $\overline{K}$ reaches a minimum at some crack length which represents the point of transition from short to long crack behaviour. Beyond this crack length $\overline{K}$ starts to increase approaching a linear relationship as a/h becomes large. This implies that the applied force gradually increases up to a peak value at the corresponding to $\overline{K}$, will be denoted $\overline{H}$ and the corresponding crack length and resultant force, $\overline{a}$ and $\overline{P}$, respectively. As the load ratio increases, $\overline{H}$ decreases. This implies that a blade configuration that induces a higher ratio of vertical to horizontal cutting forces requires less draft to cause soil failure by brittle fracture. In general, for load ratios V/H from 0.15 to 0.8, K_I initially decreases to a minimum and then subsequently increases rapidly until $\overline{K}$ almost entirely comprises K_I *ie* $K_{II} \cong 0$. This agrees with the analysis by Cotterell *et al*. (1985) of a long crack propagating parallel to the free surface. K_{II} is seen to decrease gradually at first and then rapidly, until it attains a value of approximately zero for long

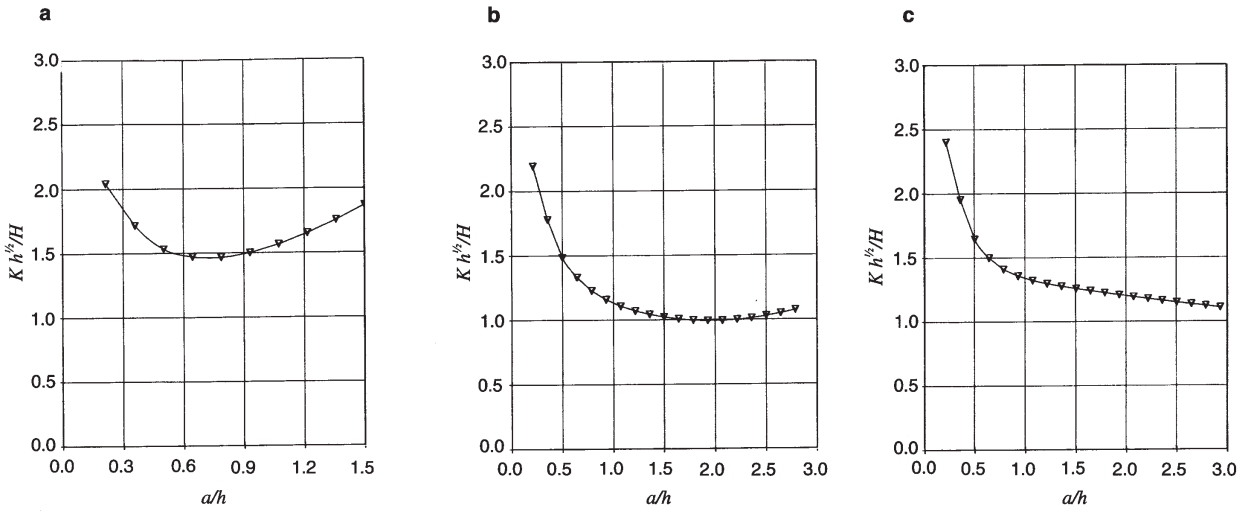

Fig. 10. Preliminary curves of the modulus $\overline{K}$ of the applied stress intensity factor for short and long crack regimes: a – $V/H = 0.5$, b – $V/H = 0.2$, c – $V/H = 0.05$.

transition point. The applied force then falls off with further crack extension. For a V/H of 0.05, $\overline{K}$ is seen to decrease monotonically and, within the practical range of crack lengths considered, no transition point occurs. This suggests that the applied force continues to increase as the crack grows. The implication of this will subsequently be discussed in the light of the pattern of K_I.

Figure 11 shows a typical comparison of the stress intensity factors $\overline{K}$ obtained using the *CRACK.TIP* module and those obtained using Eqs (3), (4) and (5) (interpolation procedure) for an arbitrarily chosen load ratio V/H of 0.2. The figure shows very good agreement between the two curves of $\overline{K}$, the slight difference being attributed to the interpolation procedure used in the first method.

Typical examples of the stress intensity factor solutions obtained using the *CRACK.TIP* module procedure are shown in Fig. 12. As expected, $\overline{K}$ generally exhibits the same trends in Fig. 12 as earlier seen in Fig. 10 and a transition point, from short to long crack behaviour, can be identified for each load ratio V/H. The peak force applied at this point,

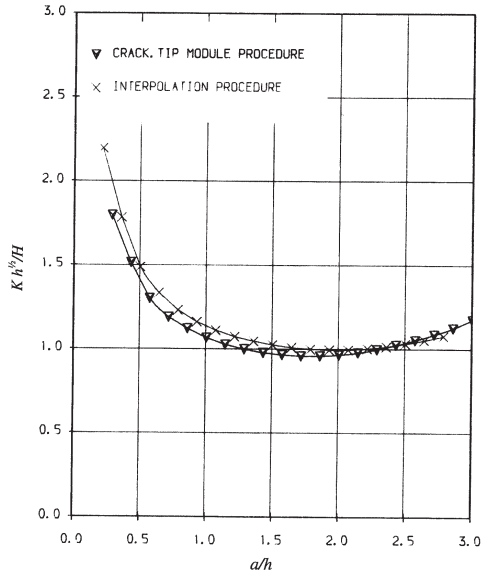

Fig. 11. Comparison of stress intensity factors $\overline{K}$ from two different FEM procedures: $V/H = 0.2$.

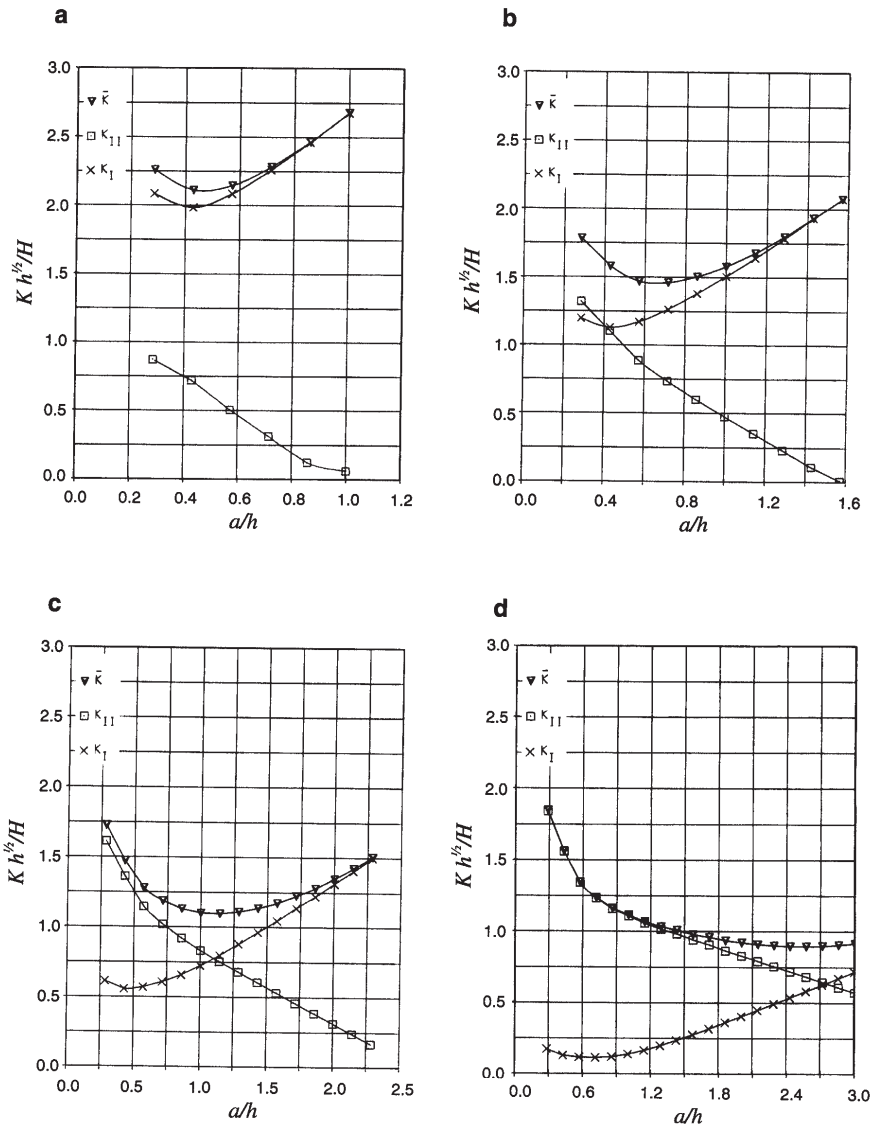

Fig. 12. The complete stress intensity factor curves for different load ratios: a – $V/H = 0.8$, b – $V/H = 0.5$, c – $V/H = 0.3$, d – $V/H = 0.15$.

crack behaviour. Its main effect on the developing crack is to affect the direction of the crack path by either causing an intra-flexion or causing the crack to turn off towards the free surface (Cotterell *et al*., 1985). The crack length at the transition point of the K_I curve will be denoted a_I and the corresponding peak force, H_I. The resultant force corresponding to a_I will be denoted P_I.

For low load ratios ($V/H \leq 0.15$), the pattern of K_I in the initial stages of crack growth suggests the absence of any significant crack opening. As pointed out above, in the absence of any significant crack opening tendency, if the apparently increasing applied force becomes sufficient to overcome the shear strength of the soil, shear failure rather than brittle fracture may occur. This agrees with the findings of Aluko and Chandler (2004) who analysed Eq. (1) and reported the existence of a limiting value of V/H below which brittle fracture ceases and the failure mechanism changes to shear.

Interpretation and analysis of peak force values

Further analysis of the curves of Fig. 12 indicates that two separate interpretations are possible for determining the peak values of the applied soil forces, H and V. These are based on the minimum points of the K_I and $\overline{K}$ curves and will be termed the *direct mode I* criterion and the *energy* criterion, respectively. Using the *direct mode I* criterion, the soil forces can be determined from the relationship:

$$\frac{K_I h^{1/2}}{H_I} = N_I, \tag{9}$$

and using the *energy* criterion, the soil forces can be determined from the relationship:

$$\frac{\overline{K} h^{1/2}}{\overline{H}} = \overline{N}, \tag{10}$$

where: N_I and $\overline{N}$ are constants obtained from the non-dimensional plots of Fig. 12. N_I and $\overline{N}$ will be termed the N-factors. The variation of the N-factors can be represented on a non-dimensional plot for various load ratios as shown in Fig. 13. If K_{Ics} is known, then for a particular *V/H*, H_I and $\overline{H}$ can be determined first by obtaining N_I and $\overline{N}$ from Fig. 13, and then using Eqs (9) and (10). The transition crack lengths a_I and $\overline{a}$ are represented on a non-dimensional plot (Fig. 14) as functions of the ratio of applied loads *V/H*. Values of critical crack length a_c predicted using the equation (Aluko and Chandler, 2004):

$$a_c = \frac{2Hh}{3V}, \tag{11}$$

are also plotted in Fig. 14. It can be seen that a_c is greater than $\overline{a}$ by a constant factor of 2 over the range of load ratios indicated whilst little or no change occurs in the value of a_I.

Brittle fracture force estimation

It has been pointed out (Aluko and Chandler, 2004, 2006) that the two major inputs required for the estimation of brittle fracture cutting forces are the soil critical stress intensity factor K_{Ics} and the ratio *V/H* of the vertical and horizontal components, respectively, of the applied cutting force *P* (Fig. 1). As a first approximation, input values of *V/H* for the present brittle fracture force prediction were empirically determined from published *V/H* versus rake angle curves (Aluko and Seig, 2000). Furthermore, K_{Ics} values were obtained from the data published by Aluko and Chandler (2006).

Using the *direct mode I* and *energy* criteria discussed above, brittle fracture force prediction was carried out for soil and blade conditions corresponding to the experimental conditions previously reported by Aluko and Seig (2000). In Fig. 15, measured (Aluko and Seig, 2000) and predicted (passive pressure theory and brittle fracture theory) resultant soil cutting forces are compared for polished blades in sandy loam and clay loam soils. It can be seen that, in general, brittle fracture force prediction using the energy criterion (Eq. (10)) produces greatly underestimated values in comparison with the experimentally measured forces. For example, in Fig. 15a the predicted resultant forces $\overline{P}$ are approximately between 39 and 43% of the measured forces.

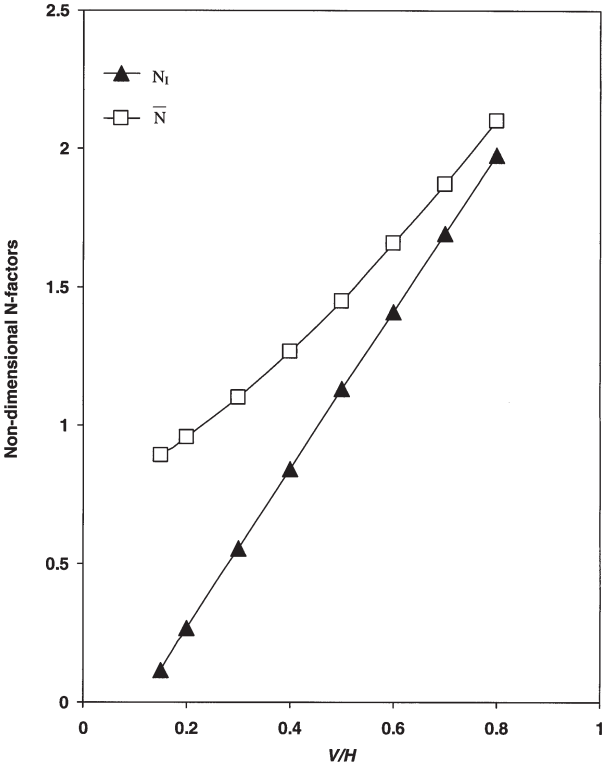

Fig. 13. N-factor curves for different load ratios *V/H*.

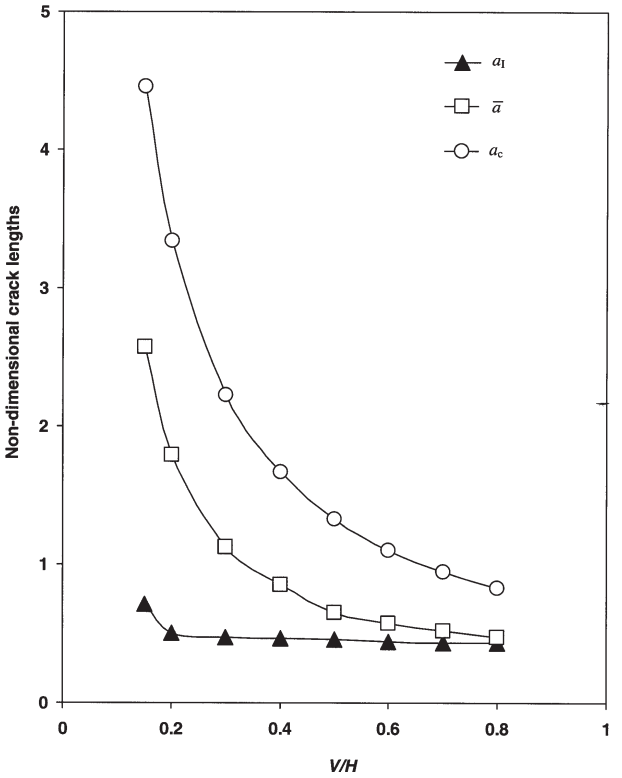

Fig. 14. Theoretical critical and transition crack lengths for different load ratios *V/H*.

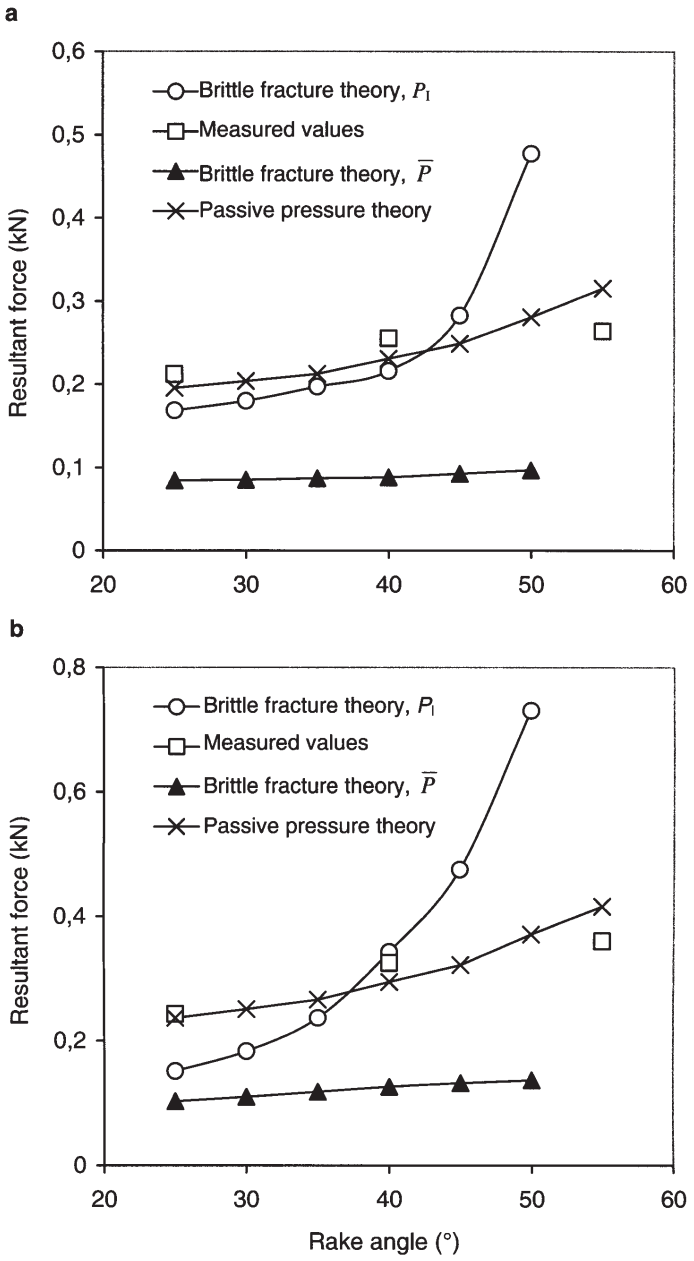

Fig. 15. Measured and predicted forces on polished cutting blades in: a – a sandy loam soil ($\omega = 176.0$ g kg^{-1}, $c = 16.00$ kN m^{-2}, $\phi = 35°$, $K_{Ics} = 3177.73$ N m$^{-3/2}$) and b – a clay loam soil ($\omega = 234.7$ g kg^{-1}, $c = 18.38$ kN m^{-2}, $\phi = 40°$, $K_{Ics} = 4522.71$ N m$^{-3/2}$). ω is the soil moisture content; c is the cohesive strength of the soil; ϕ is the angle of internal shearing resistance of the soil; K_{Ics} is the soil critical stress intensity factor.

However, when the direct mode I criterion is used, the predicted brittle fracture forces P_I show reasonable agreement with the measured forces for a limited range of rake angles. For most soils, the predicted resultant force P_I initially increases gradually as the rake angle increases. At some rake angle, the pattern changes drastically and P_I rapidly increases to very high values. This trend in the curves of P_I (Fig. 15) is a consequence of low V/H values as the rake angle is increased.

A criterion for predicting which type of failure will occur in a given situation entails consideration of the force required for the alternative failure mechanisms. This criterion, termed the *minimal energy* criterion, assumes that whichever of the two failure mechanisms *ie* shear failure or brittle fracture requires the lesser force will occur in a given situation. For the sandy loam soil (Fig. 15a), application of the minimal energy criterion indicates that brittle fracture (using P_I) would occur for a 40° raked blade and shear

failure would occur for a 45° raked blade. The theoretical failure transition rake angle would be about 43°. This agrees with previously published (Aluko and Seig, 2000) experimental results for polished blades in the sandy loam soil. For the clay loam soil (Fig. 15b), on the other hand, the theoretical failure transition rake angle *ie* from brittle fracture to shear failure can be seen to be about 37°. However, during soil cutting experiments with polished blades in this clay loam soil (Aluko, 1988; Aluko and Seig, 2000), cutting with a 40° raked blade produced brittle fracture whilst cutting with a 55° raked blade produced shear failure. This suggests that specifying a limited failure transition rake angle (or *V/H*) range may be more appropriate in the application of the *minimal energy* criterion to failure type prediction rather than an abrupt failure transition rake angle value.

CONCLUSIONS

1. The finite element method has been used successfully to resolve the major limitation of the brittle fracture theory developed by Aluko and Chandler (2004), namely the deduction of short crack behaviour under mixed mode loading. Consequently, for load ratios $V/H \geq 0.15$, there is a smooth transition from short to long crack behaviour rather than an abrupt change in the level of the applied stress intensity factor.

2. The present further development of the brittle fracture model leads to two possible interpretations for estimating peak soil cutting forces. These have been termed the *direct mode I* criterion and the *energy* criterion. Whilst the *energy* criterion significantly underpredicts the resultant force, the *direct mode I* criterion gives reasonable force estimates compared to measured values over a limited range of low rake angles. The model demonstrates that at low values of *V/H*, the cutting force required for brittle fracture becomes very large. In practical terms, this is brought about by changes in blade configuration.

3. Based on the comparison of predicted forces from both passive pressure theory and the brittle fracture model, a minimal energy criterion is proposed which provides a way of predicting the expected failure mechanism in a given situation.

4. At present, only empirical methods are available for the determination of *V/H*, which is a major input to the model.

REFERENCES

Aluko O.B., 1988. Brittle fracture in soil cutting. Ph.D. Thesis, University of Newcastle upon Tyne, UK.

Aluko O.B. and Chandler H.W., 2004. Characterisation and modelling of brittle fracture in two-dimensional soil cutting. Biosys. Eng., 88(3), 369-381.

Aluko O.B. and Chandler H.W., 2006. A fracture strength parameter for brittle agricultural soils. Biosys. Eng., 93(2), 245-252.

Aluko O.B. and Seig D.A., 2000. An experimental investigation of the characteristics of and conditions for brittle fracture in two-dimensional soil cutting. Soil Till. Res., 57, 143-157.

Anonymous, 1990. Plaxis – Finite Element Code for Soils and Rock Plasticity. Version 3. Balkema Press, Rotterdam, the Netherlands.

Bofinger H.E., 1970. The Measurement of the Tensile Properties of Soil-Cement. RRL Report LR 365, Ministry of Transport Press, Berkshire, Australia.

Chi L. and Kushwaha R.L., 1987. Three-dimensional finite element analysis of soil failure under a narrow tillage tool. ASAE Paper No. 88-1582, St. Joseph, MI, USA.

Chi L. and Kushwaha R.L., 1989. Finite element analysis of forces on a plane soil cutting blade. Can. Agric. Eng., 31, 135-140.

Coleman G.E. and Perumpral J.V., 1974. The finite element analysis of soil compaction. Transactions of the ASAE, 17, 856-860.

Cotterell B., Kamminga J., and Dickson F.P., 1985. The essential mechanics of conchoidal flaking. Int. J. Fracture, 29, 205-221.

Fielke J.M., 1999. Finite element modelling of the interaction of the cutting edge of tillage implements with soil. J. Agric. Eng. Res., 74, 91-101.

Henshell R.D., 1984. PAFEC Theory Manual. PAFEC Press, Nottingham, UK.

Liu Yan and Hou Zhi-Min, 1985. Three dimensional nonlinear finite element analysis of soil cutting by narrow blades. Proc. Int. Conf. Soil Dynamics, Auburn, AL, USA, 2, 322-337.

Perumpral J.V., Liljedahl J.B., and Perloff W.H., 1971. The finite element method for predicting stress distribution and soil deformation under a tractive device. Transactions of the ASAE, 14(6), 1184-1188.

Raper R.L. and Erbach D.C., 1990. Prediction of soil stresses using the finite element method. Transactions of the ASAE, 33(3), 725-730.

Seig D.A., 1985. Soil compactability. Ph.D. Thesis, Institute of Technology, Cranfield, UK.

Yong R.N., Fattah E.A., 1976. Prediction of wheel-soil interaction and performance using the finite element method. J. Terramechanics, 13, 227-240.

Yong R.N. and Hanna A.W., 1977. Finite element analysis of plane soil cutting. J. Terramechanics, 14(3), 103-125.

Zienkewicz O.C., 1971. The Finite Element Method in Engineering Science. McGraw-Hill Press, London, UK.